Evaluation of fracture toughness of cartilage by micropenetration

N. K. SIMHA
University of Miami, Miami, FL, USA

C. S. CARLSON, J. L. LEWIS*
University of Minnesota, Minneapolis, MN, USA
E-mail: lewis001@umn.edu

Failure properties of cartilage are important in injury repair and disease, but few methods exist for measuring these properties, especially in small animals. To meet this need, a new indentation/penetration method for measuring fracture toughness of cartilage is proposed. During indentation, a conical tip is displaced into the surface of the cartilage, causing first a non-penetrating indentation, and then a penetration into the tissue. The method assumes that tissue penetration occurs during periods of ''rapid work'', which are identified from a curve of work rate vs. time. Total penetration depth is determined by summing the displacement during these periods. Fracture work is the work that occurs during ''rapid work'', or penetration, and fracture toughness defined as the fracture work divided by one-half the penetrated surface area of the indenting tip.

The method was validated by indentation testing of bovine cartilage. Penetrating indentations with a conical tip were performed in bovine patellar cartilage and depth of penetration and fracture toughness predicted. For comparison with the indentation data, depth of penetration was measured in histological sections. These measurements agreed well with the predicted depth. Predicted fracture toughness also agreed with values measured via a macroscopic test. This newly described method has promise as a general method for measuring fracture toughness in cartilage, particularly in small animals, since penetrating tips with small tip radius can be manufactured and penetration may be accomplished in cartilage of minimal thickness.

Introduction

Failure properties of cartilage are important in injury repair and disease, but few methods have been developed for their measurement [1–3]. Tensile strength is the most common method used [4–6], however, it does not simulate the failure mechanism of cartilage. Since cartilage fails by fibrillation and crack formation [7, 8], a fracture or crack propagation approach would seem more appropriate. In addition, preparation of small, regularly shaped specimens is required for tensile [4] and conventional fracture tests [1–3], and this is difficult in small animals where a small volume of cartilage tissue is available. In this paper, a novel micropenetration method is proposed for measuring the fracture toughness of articular cartilage. The method creates a penetration or fracture defect in the surface of intact cartilage that is attached to underlying subchondral bone and does not require the preparation of small, regularly shaped specimens. Because of the small indenting tips used, the technique has a resolution on the order of tens to hundreds of microns. Although the Nanoindenter XP (MTS, Inc.) instrument is used in the present study, indentation depths are on the order of 100 μm, which are considerably larger than those used in conventional nanoindentation methods [9], hence the proposed methods are termed ''micropenetration''.

Nanoindentation has become a useful tool for determining the Young's modulus and hardness of relatively hard materials such as metals [9]. In these indentation tests, a relatively sharp tip of predetermined geometry is pressed into the material to a certain depth and then retracted, while load and displacement are measured. During loading, a metal specimen primarily undergoes plastic deformation, whereas during unloading the metal recovers predominantly by elastic recoil. In most studies, the penetration depth and stiffness are deduced from the unloading data, and from these, the Young's Modulus and hardness are determined.

The established nanoindentation methods evolved from traditional hardness testing. Hardness is defined as the maximum force applied to an indenter divided by the projected area of the impression at maximum force. Conventional hardness tests require measuring the size of

*Author to whom all correspondence should be addressed: Mayo Mail Code 289, 420 Delaware Street, S.E. Minneapolis, MN 55455.

the impression after the test. This procedure is especially useful for materials that deform plastically, since an impression remains after the test, and the impression left is directly related to the geometry of the indenting tip. It has always been clear that hardness is not a material property, since it strongly depends on the shape of the indenter. However, the hardness test is simple, requires minimal specimen preparation, and is useful on a comparative basis. In addition, for certain conditions, hardness numbers of materials can be correlated to material properties (e.g. ultimate strength in MPa = 3.45 × Rockwell B hardness for most steels). Hence, hardness tests have been extensively used.

With the development of instrumented-indentation techniques, Doerner and Nix [10] proposed methods to determine the area of the impression from force–displacement data and tip geometry, without the need to directly view the impression. The essential step is to determine the inelastic penetration depth of the indent, from which indent projected area can be determined using the geometry of the tip. Penetration depth is the difference between the measured total displacement and the recoverable elastic displacement. Doerner and Nix [10] proposed that the elastic displacement be determined by assuming that unloading from the maximum load is essentially elastic and, at maximum load, the penetrated tip is equivalent to a flat ended indenter of area equal to the penetration projected area. From measurement of the actual stiffness at initial unload, extrapolation along this stiffness curve back to zero load gives the elastic displacement at maximum load. This is then subtracted from the total displacement to give the inelastic deformation at maximum load. From the inelastic displacement and the tip geometry, the projected area of the indenter at maximum load can be determined. In conjunction with a theoretical linear elasticity solution for a flat ended indenter on a half space, the stiffness at maximum load can also give a value for the Young's modulus, assuming a value of Poisson's ratio and isotropic material.

Oliver and Pharr [9] showed that this procedure must be altered to account for the deviation of the actual indent from the theoretical solution for a flat-ended cylindrical indenter. Actual indenters are conical or prismatic and do not behave as a flat ended cylinder on unloading. They assume that the stiffness at maximum load is due to the conical or prismatic tip indented elastically into a flat surface. They then use the form of the elastic solution for stiffness for that tip geometry to deduce the defect surface area and, from this, the hardness. Elastic modulus is not needed for this procedure. To deduce elastic modulus, or $E^* = E/(1 - \nu^2)$, the elastic solution for that tip geometry is used again at unloading from maximum load. Oliver and Pharr [9] use only elastic solutions for their tip geometries. An essential assumption in their method is that the elastic unloading of a flat surface is the same as the elastic unloading of a surface with a permanent indent. Since they use tips with large included angles, such as the Berkovitch tip, on metal surfaces with plastic defects, this assumption is reasonable and they get good predictive results with their methods for relatively stiff materials such as metals and ceramics.

Our experience with indenting cartilage indicates that there are fundamental differences between nanoindentation testing of soft tissues, such as cartilage, and metals (unpublished data). During nanoindentation of metals, there is a negligible elastic displacement regime at low loads followed by elasto-plastic deformation during the majority of loading. In contrast, when cartilage is indented with a sharp indenter, the initial deformation is primarily viscoelastic and the viscoelastic displacement can be up to 200 μm. It is difficult to penetrate the material. However, after a critical value of load is reached, the indenter tears the surface of the cartilage and penetrates the tissue, generating a crack-like defect. Hence, a combination of viscoelastic deformation and penetration by crack propagation is primarily observed at higher loads in cartilage. There is no evident plastic deformation.

Because of these fundamental differences between the defect mechanisms – tearing in cartilage and plasticity in metals – the standard methods for hardness and nanoindentation cannot be extended to cracking of soft tissues. First, the large viscoelastic deformations for soft tissues means that the slope of the unloading curve is time dependent and can be negative for slower loading rates. Second, the tear closes upon unloading. Finally, because tips with smaller included angle are necessary to achieve penetration, the equivalence of the indentation of the material with penetration defect and a flat surface becomes unrealistic. A different method is needed that accounts for the time dependency, larger penetration depths, larger deformations, and tissue fracture. Such a method is proposed in the present paper.

The method is based on identification of regions of penetration during indentation. A first critical step in the proposed method is the prediction of the penetration depth during tearing, as opposed to the total displacement of the indenter. A second critical step is to determine the fracture work during the tearing process, independent of other non-fracture work. In this paper, methods are proposed for determining the penetration depth, fracture work, and fracture toughness for cartilage and similar soft materials, during indentation/penetration testing.

It is important to distinguish between the proposed methods here and previously described methods used in cartilage research that may appear to be similar. It is well known that tears can be introduced on the surface of cartilage by the use of sharp pins, producing the so called ''split lines'' [11]. The method proposed here produces tearing at much more shallow penetrations that generally do not create ''split lines''. Another source of potential confusion is that, although non-penetrating indentation has been used extensively to study cartilage [12], most studies have used flat-ended cylindrical [13] or spherical indenters [12] and have evaluated the prefailure elastic and viscous properties. The novel feature of the proposed methods is that a conical indenter tip is used to specifically examine the failure properties of cartilage.

There is no consensus on the terminology for a penetration process in a soft material. This process may be considered a Mode I crack propagation, quantified as work done per unit of crack area, and defined as fracture toughness [14]. This may cause confusion, since the term ''fracture toughness'' is used mainly with metals and associated with K_{Ic} of linear elastic fracture mechanics or

similar parameters. Alternatively, the soft tissue failure could be considered to be tearing and quantified as a tear test, such as a trouser tear test [14]. This is also a work done per unit of new area, but the work is done in Mode III, rather than Mode I. It would seem the micropenetration process conforms more to the Mode I crack process, so in this paper the process will be defined as fracture toughness. We believe this is consistent with the convention adopted by Atkins and Mai [14].

Materials and methods

The Nanoindenter XP (MTS, Inc., Minneapolis, MN) was used to indent bovine articular cartilage from the patella. The instrument consists of an indentation tip driven in the vertical direction by a controlled force. Vertical force and displacement are measured during the indentation. A small amplitude harmonic displacement (2 nm at 45 Hz) is superimposed on the quasistatic motion to allow instantaneous stiffness to be determined, independent of the quasi-static stiffness. The resolution of the Nanoindenter XP is about 0.1 mN for the force applied by the indenter and about 0.1 μm for indenter displacement. The sample is mounted on an *x*–*y* stage for which motion can be measured and controlled in microns.

Bovine patellae were obtained from a local slaughterhouse within a few hours of slaughter and frozen. Just prior to testing, they were thawed and specimens approximately $10 \times 10 \times 4\,\text{mm}^3$ (including the entire thickness of articular cartilage, which was 1–2 mm thick) were cut from the patella. A flat layer of subchondral bone was left on each specimen, and the specimen was attached by bonding the bone to a holder with cyanoacrylate cement. A special holder was used that allowed rotation of the specimen surface to make the tip motion perpendicular to the cartilage surface. A bead of phosphate buffered saline (PBS) was placed on the specimen surface, which was moved into position by adjusting the *x*–*y* motion to choose the site of indent.

Standard protocols for the Nanoindenter XP that were designed for indenting hard materials were modified for soft tissues. Prior to the indentation test, the tip must first be brought into unloaded contact with the surface, and then the formal indent protocol performed. To find the surface, the indenter tip is positioned a relatively large distance away and then made to approach the surface while monitoring stiffness. When the surface is encountered, there is a dramatic rise in stiffness. With soft tissues, this change in stiffness is much less dramatic and may amount to little more than the system noise. To account for this, the surface was first estimated during loading by an increase in harmonic stiffness (from the superimposed 45 Hz displacement), and then refined by unloading at a slower rate to the point of load removal. After finding the surface, the indent was performed at a constant loading rate to a maximum load. The load was held for 10 s, and then removed at constant load rate. A diamond conical tip with a 67° included angle was used; the tip was truncated, with a flat end of approximately 10 μm diameter.

Four different specimen groups were tested (Group 1: identify penetration; Group 2: compute fracture toughness; Group 3: repeat of Group 2; Group 4: repeat of Group 2 and penetration depth by histology). One of the difficulties in indenting soft tissues is determining whether penetration has occurred. Therefore, a first set of indents (Group 1) was performed to assess ability to identify penetration from the instrument data. Preliminary testing suggested that power, or work rate, may be a sensitive indicator of penetration. Power is defined as

$$P(t) = F(t)\Delta h/\Delta t \tag{1}$$

where F is the indenting force, h is the indentation depth, and t is the time.

The rationale for the choice of this parameter is that the work rate is relatively smooth for a constant loading rate when there is no penetration, but increases abruptly when greater work is done on penetration. For this test set (Group 1), seven indents with maximum loads of 75, 125, 150, 200, 300, 400 and 400 mN, respectively, were performed on a bovine cartilage specimen at a loading rate of 4 mN/s. To verify penetration, the specimen was stained with India ink after testing and examined under an optical dissecting microscope. Penetration was identified by localization of India ink in the created defect.

The Group 1 tests demonstrated that penetration occurred at load levels of 300 and 400 mN. Therefore, on a second cartilage specimen six indents in a 3×2 pattern 300 μm apart were performed, three at 300 mN and three at 400 mN maximum load, at a loading rate of 4 mN/s (Group 2). After testing, the specimen was stained with India ink and examined under a dissecting microscope. To assess repeatability, a second specimen was tested by the identical protocol (Group 3). An additional specimen (Group 4) was indented by the same procedure and then was decalcified in 10% EDTA, dehydrated, and embedded in paraffin. This specimen was serially sectioned at 4 μm intervals, with sectioning being initiated proximal to the point where defects were grossly visible and ending beyond the site where no defect was grossly evident (approximately 300 sections). Serial sections were stained with hematoxylin and eosin and each section was digitized and the depth of the penetration quantified using the software package ImageJ (image analysis software based on NIHImage, available at http://rsb.info.nih.gov/ij/index.html).

To provide a standard of a material that does not penetrate, and to aid in interpreting the cartilage data, a urethane rubber (Measurements Group, Raleigh, NC, type SB-4B) specimen of thickness 2 mm, glued to a substrate, was indented with the same tip and loading rate to 400 mN maximum load. Urethane rubber has an elastic modulus of the same approximate value as cartilage, but it is not penetrated at up to 400 mN maximum load with the tip used on the cartilage.

The cartilage penetration depth was predicted from the load–displacement data by assuming that the mechanical power changes rapidly during penetration (see Results, Fig. 5), and that all displacement that occurs during the corresponding time period is penetration displacement. The rationale for using power as the indicator for penetration is that, for a constant loading rate, work rate, or power, should be relatively smooth, reflecting the

gradual absorption of elastic and viscous energy. When penetration occurs, not only elastic work is being performed, but fracture work is being done as well, leading to an increase in work rate. The first rapid increase in power will correspond to the initiation of penetration. Subsequently, if the power rate (PR) and power (P) are elevated in comparison to the values for a non-penetration standard, then penetration occurs during such time instants as well. For the cartilage specimens, this non-penetrating curve (P_{fit}) was estimated by curve fitting the region up to the first penetration, and then extrapolating the curve fit over the entire indent range. The curve fitting function of power vs. time was

$$\text{Power fit} = P_{fit} = y_0 + A_1 e^{-t/t1} + A_2 e^{-t/t2} \qquad (2)$$

This choice of function will be supported by comparison with the urethane rubber response. The non-penetrating power rate (PR_{fit}) was determined by differentiating this function. Penetration was assumed to occur when the power rate (PR_{test}) was elevated and the power (P_{test}) was above the value for no penetration:

$$|P_{test} - P_{fit}| > F = 13\,000\,\text{mN nm/s}$$

and

$$|PR_{test} - PR_{fit}| > H = 5000\,\text{mN nm/s}^2 \qquad (3)$$

H and F are parameters greater than zero introduced to account for noise in the signal. Differences in Equations 3 must be greater than H and F in order to be considered penetration. Justification for choice of H and F values will be described in the Discussion section. These criteria were evaluated at each time point and all penetration increments satisfying these criteria summed to give total penetration. The data reduction process was implemented within an Excel (Microsoft, Inc.) spreadsheet.

Total work done during the loading phase of the indent was divided into the non-fracture and fracture work. The fracture work was computed as the work done during the penetration time periods. The work during penetration was then calculated according to the following formula:

$$\text{Penetration work} = W_p = \int F\,dh_s \qquad (4)$$

where h_s is the displacement during penetration.

Fracture toughness is proposed as a measure of the resistance of the tissue to penetration. The fracture toughness is defined as the ratio of the penetration work, W_p, to one-half the surface area of a cone with depth h_{pen}, the total penetration depth. The factor of one-half conforms with standard practice in fracture mechanics to describe crack area as the projected area, which would be one-half the new surface area. For a cone with apex included angle α, the fracture toughness can be written as

$$T = \frac{W_p \sqrt{2}}{\pi h_{pen}^2} \frac{(1+\cos\alpha)^{3/2}}{\sin\alpha} \qquad (5)$$

Results

A comparison of the load versus displacement graphs for the six cartilage indents in Group 2 and the urethane rubber sample show there is negligible energy dissipation

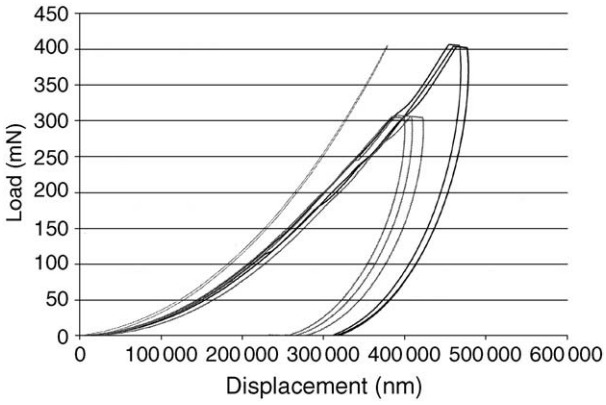

Figure 1 Load–displacement curves for indents in cartilage and urethane rubber with 67° conical diamond tip. Three indents to 300 mN maximum load and 3–400 mN maximum load at a loading rate of 4 mN/s were made in bovine patellar cartilage and one indent in urethane.

for the urethane rubber and considerable dissipation in the cartilage (Fig. 1). Although only one urethane rubber test is shown, there was good reproducibility for this test (data not shown). There is also good reproducibility for the cartilage at the two maximum loads, although there is some shifting of the curves along the time axis in Fig. 1 due to variations in locating the surface. Careful observation reveals that several perturbations in slope are present in the loading part of the cartilage force–displacement curves. Such perturbations are not present in either the urethane or the unloading part of the cartilage curves. Except for these perturbations, the curves are relatively smooth. It is possible that the perturbations correspond to penetration. Indeed, penetrations were observed in each of these specimens, as can be seen in the India ink stained images for the six indents in Group 3 (Fig. 2). All six penetrations are visible and it is clear that the 400 mN indents create larger defects than do the 300 mN indents, as would be expected.

Although there are indications of penetration in the force–displacement curves, preliminary data showed that work-rate was a much clearer indicator of penetration. To assess this, a cartilage sample was indented with a series of indents with increasing load (Group 1) and compared with India ink staining. The power for these as a function of time during loading are shown in Fig. 3. Penetration is hypothesized to occur when there is a rapid change in power. By this criterion, it appears that indents above and including 150 mN penetrated. The India ink images of these and additional indents are shown in Fig. 4. It is evident that these were the indents that penetrated, and the 125 mN indent did not penetrate, supporting the use of change in power as a criterion for penetration.

The power versus time for three cartilage indents and the scaled urethane rubber is shown in Fig. 5. The smoothed power rate for the urethane and one cartilage test are shown in Fig. 6. The urethane data in Fig. 5 was fit using Equation 2, differentiated, and also is shown in Fig. 6, as is the cartilage data prior to 26 s, which was fit in a similar manner. The data in Figs. 5 and 6 were subjected to the criteria in Equations 3, so that whenever power rate for the cartilage was above that of the fit power rate curve by $H = 5000\,\text{mN nm/s}^2$ and the power was above the fit power curve by $F = 13\,000\,\text{mN nm/s}$,

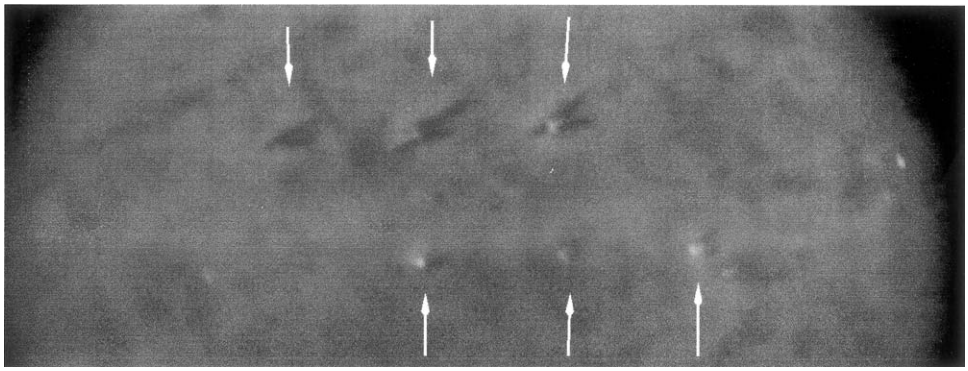

Figure 2 Surface defects (arrows) produced by 300 mN (bottom row of three) and 400 mN (top row of 3) maximum load indents with 67° conical tip in bovine cartilage, stained with India ink and observed in a dissecting microscope. Indents are 300 μm apart.

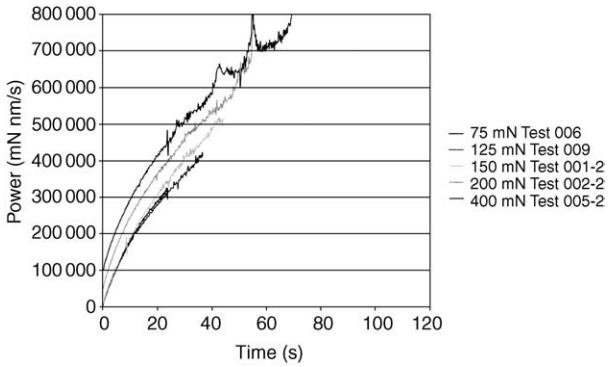

Figure 3 Power (work rate) for five indents in bovine cartilage to differing maximum load. Note deviation from smooth curve for 150 mN and higher. This is interpreted to indicate penetration. Curves for 200 and 400 mN have been artificially placed higher on the power scale for clarity.

that displacement was assumed to be penetration, and the work done assumed to be penetration work. These predicted penetrations and work were summed for all time steps that satisfied the criteria in Equation 3 to give total predicted maximum penetration and fracture work. The predicted maximum penetration depths for each of six indents in cartilage for test Groups 2 and 3 are shown in Fig. 7 and in Table I.

A typical histology image for an indent in Group 4 is shown in Fig. 8, along with the measure of penetration depth for one defect. The penetration depths measured from the histological sections are shown in Fig. 9. Only values from sections having penetration depths similar to those in three or greater adjacent sections were used. This allowed elimination of values from sections in which vertical tearing of the defect area occurred artifactually during sectioning. From the measured values, the maximum penetration depth for each of the six indents was estimated (Table I). The penetration depths measured from the histological sections were not significantly different from the predicted penetration values (*t*-test, Fig. 7 and Table I).

The fracture toughness was calculated as described above for the two sets of six indents in cartilage test Groups 2 and 3 (Table II and Fig. 10). For comparison, fracture toughness of bovine patellar cartilage as measured by Adams *et al*. [15] using the modified single edge notch test (MSEN) of Chin-Purcell and Lewis [3] is also shown (Table II and Fig. 10), as is the fracture toughness for canine patella cartilage measured using the MSEN test [3] (Table II). The average fracture toughness from the present study was not significantly different from that measured by Adams *et al*. [15] (Student's *t*-test).

Discussion

The goal of this work was to develop and demonstrate methods for penetrating cartilage and predict the fracture toughness using a micropenetration technique. This goal was accomplished, as the predicted fracture toughness using this newly described method was not significantly different from that measured by a macroscopic test. The predicted penetration depths were also not significantly different from those directly measured in histological sections. The penetration depths were up to 250 μm,

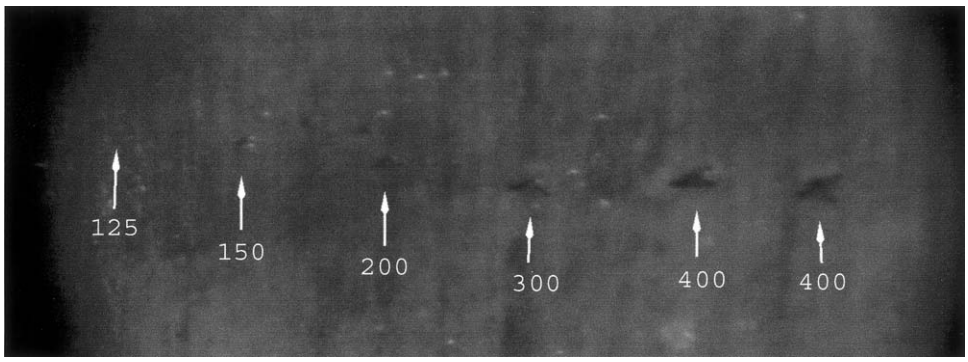

Figure 4 Surface defects produced by indents of differing maximum load (maximum load in mN indicated with arrows). Penetration occurred for 150 mN and above. There is no apparent defect due to the 125 mN indent, in agreement with Fig. 3 in which there is no apparent ''rapid work'' for the 125 mN power curve.

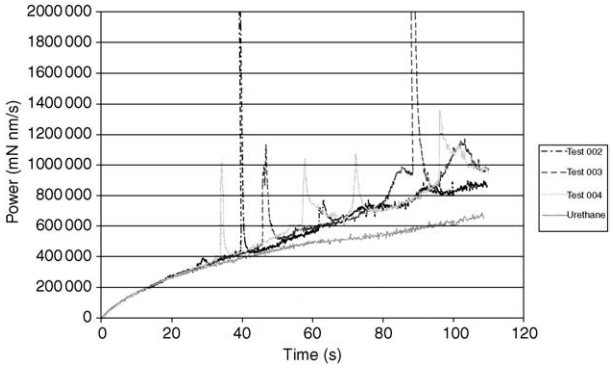

Figure 5 Power (work rate) for three identical indents (300 μm apart) to 400 mN maximum load in bovine cartilage, and one indent to 400 mN in urethane rubber. The work rate for urethane rubber has been multiplied by 0.88 to make it match the cartilage response up to the point of initial penetration (approx. 26 s). Penetration is assumed whenever the power shows rapid change, compared to the urethane curve.

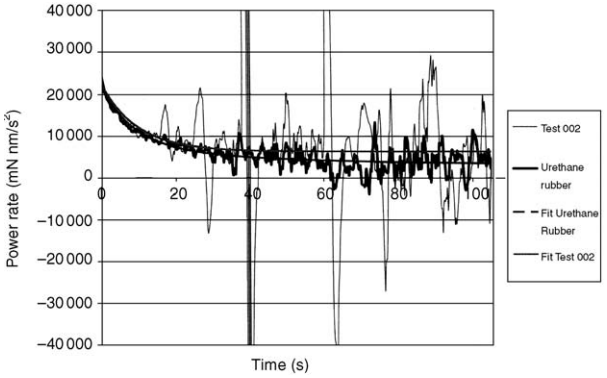

Figure 6 Power rate (rate of work rate) for cartilage Test 002 and one urethane indent from Fig. 5, and fit of urethane and Test 002 by the function in Equation 2. Penetration may occur whenever power rate of test 002 – power rate of fit test 002 $> H = 5000\,\text{mN nm/s}^2$.

considerably higher than those used in conventional nanoindentation methods on hard materials, justifying terming the new methods ''micropenetration'', rather than nanoindentation. The methods also worked well on a highly time dependent material, articular cartilage, overcoming a limitation with the conventional methods for reducing nanoindentation data.

The load–displacement curves and predicted penetration depth and fracture toughness were repeatable between tests for identical test conditions (Group 2 vs. Group 3). As one sign of internal consistency of the data,

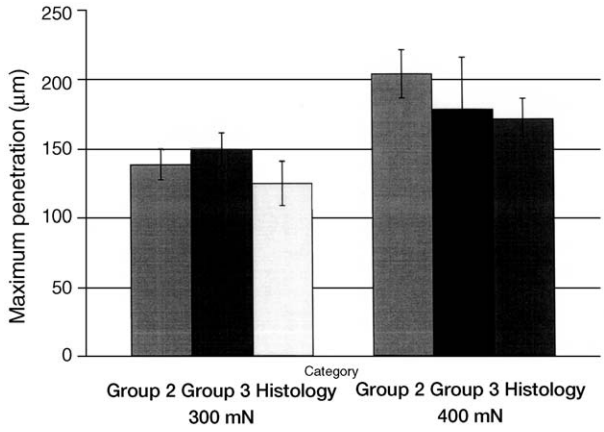

Figure 7 Penetration depth predicted from Equation 3 for Groups 2 and 3, and as measured for Group 4 by histology. Predicted penetration and penetration measured by histology are essentially the same. For each Group, $N = 3$.

the penetration depths measured for the 300 mN indents were smaller than those of the 400 mN for both groups of six indents, but the predicted fracture toughness of the 300 and 400 mN load sets within each group was identical. The mean fracture toughness was different between Groups 2 and 3 (Table II), however, this may be due to differing specimen source location. Chin-Purcell and Lewis [3] noted variation in fracture toughness with location on the canine patella.

The predicted fracture toughness compared well with available data obtained by another method. The only additional data on cartilage fracture toughness of which we are aware was generated in our laboratory using a modified single edge notch test [15]. This method requires that regularly shaped specimens from a joint surface are cut and are loaded in tension while monitoring crack extension. This is a difficult test to perform and, as evidenced by the large standard deviation in the data (Fig. 10), has considerable potential for artifact, suggesting insensitivity to small material property changes. In spite of this large variation, the Adams *et al*. data [15] is similar to the data by Chin-Purcell and Lewis [3], who tested canine cartilage using the same method. There was no statistically significant difference between the fracture toughness of bovine patellar cartilage measured by Adams *et al*. [15] and the present data.

TABLE I Maximum penetration for Groups 2 and 3 (predicted), and Group 4 (histology) evaluated by histology

Group 2			Group 3			Group 4	
Test	Max load (mN)	Max penetration (μm)	Test	Max load (mN)	Max penetration (μm)	Max load (mN)	Max penetration (μm)
2	400	136	2	400	186	400	185
3	400	194	3	400	205	400	155
4	400	204	4	400	219	400	174
Avg (SD)	178 (37)			203 (17)		171 (15)	
5	300	139	5	300	163	300	139
6	300	127	6	300	141	300	127
7	300	148	7	300	143	300	107
Avg (SD)	138 (11)			149 (12)		124 (16)	

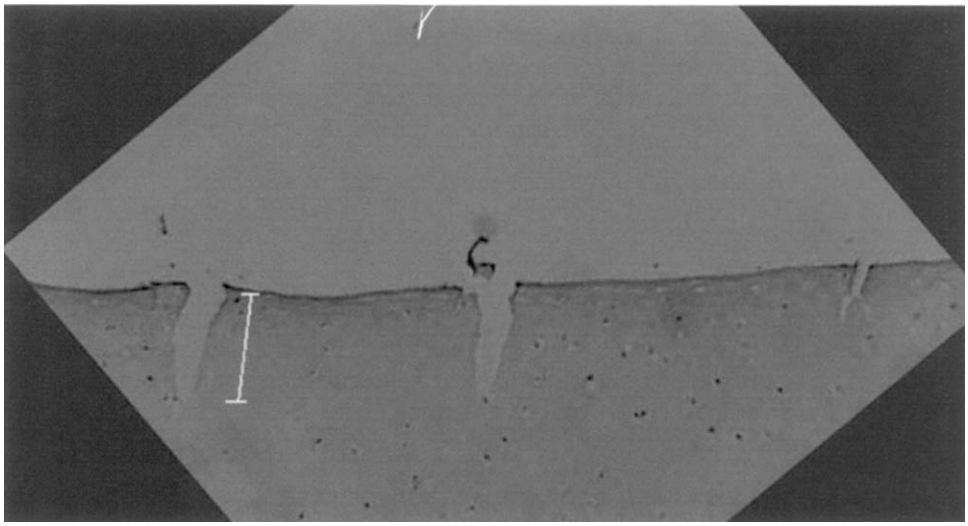

Figure 8 Histology section of bovine patellar cartilage after indentation to 400 mN maximum load by 67° conical tip, illustrating how depth of penetration was defined and measured. Indents are 300 μm apart. The bar represents the depth of penetration.

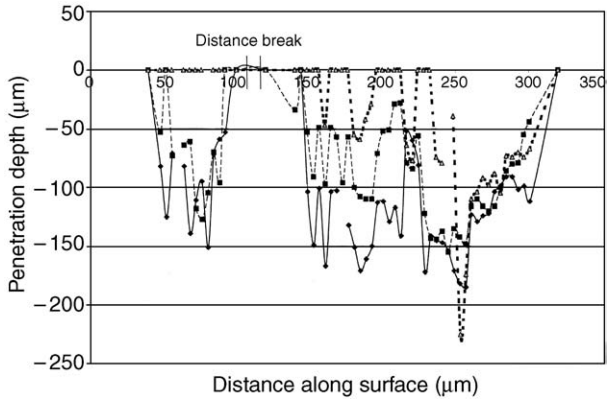

Figure 9 Penetration depth as measured from histology slides. Depth was measured from digital images of the slides using ImageJ software. Each point represents three sections. Penetrations between 0 and 100 μm are for two of three penetrations due to 300 mN; penetrations between 150 and 350 μm are due to the 400 mN indents. ''Distance break'' refers to a gap of approximately 100 μm in which there were no penetrations. The different weight curves represent single identified penetrations at the two different locations.

There are some limitations to comparison of the data from Adams *et al*. [15] with those from the present study. The MSEN test used by Adams *et al*. propagates a crack from the deep zone up toward the surface, and thus is a measure of the fracture properties of cartilage from the deep and mid-zones, not the surface. The micropenetration measurements evaluate cartilage properties near the surface, which may be different from those of the deeper cartilage.

The standard deviation (SD) of predicted fracture toughness for the indents (Table II) was significantly smaller than that reported by Adams *et al*. [15] for a macroscopic test. This is important, since it suggests that fewer micropenetration tests can determine a useful value of fracture toughness. The small SD is remarkable in that failure data for soft tissues is notoriously highly variable [5, 10]. Whether this variation reflects the non-uniformity of material tested, or the methods used is unknown. Most testing of material properties for cartilage over a joint surface has involved a fairly large (many mm's) distance. There is likely to be much less variation over the small region tested with the micropenetration method. On the other hand, there is potential for increased variation if the size of defect approaches the size of microstructural features. For the deep indents made here, this was apparently not the case.

The data indicate that the predicted penetration depth compares well with that measured in histological sections. Histology was considered to be a ''gold standard'', but this method also has drawbacks. In some sections, there appeared to be artifactual extension of the cracks, since there were occasionally large differences in crack depth between adjacent slides cut 4 μm apart. It is assumed these occurred during tissue cutting and slide preparation, since it is difficult to see how such large differences could occur during the indent. There is also the possibility of cartilage shrinkage during processing (tissue dehydration) for histology, resulting in a systematic underestimation of penetration depth. If this occurred, it would be predicted to be less than 10%.

The procedure for finding the penetration depth uses the power and power rate vs. time curves for the case of no penetration during indentation at constant loading rate. The shape of these curves is not obvious beforehand and the choice of fitting function needs justification. To justify the procedure used, the power and power rate vs. time data were obtained during indentation of urethane rubber, which does not undergo penetration even at the higher load level of 400 mN. Plotting the cartilage data and urethane data on the same power versus time plot shows that the curves during the non-penetrating time are very similar, appearing to differ by a scale factor. Hence, the urethane rubber power was multiplied by a constant to bring the urethane power curve into close agreement with the curve for cartilage during this non-penetrating range. The urethane curve of power vs. time was fit with Equation 2, and differentiated to give fit power rate vs. time. The fit power curve for urethane agrees very well with the cartilage fit curve even for larger load levels, suggesting that the extrapolation of the cartilage fit curve is a reasonable way of estimating the non-penetrating cartilage curve. The variations in this fitting function are mainly in the magnitude of the power, not in the power rate. Penetration is assumed to occur when the power and power rate are greater than some limit, which accounts

TABLE II Fracture toughness of bovine cartilage by micropenetration for Groups 2 and 3, and comparison values

Test	Max load (mN)	Fracture work (Nm)	Area m^2	Fracture toughness (Nm/m^2)
Group 2				
2	400	3.03E-05	2.29E-08	1322
3	400	5.25E-05	4.68E-08	1121
4	400	4.78E-05	5.18E-08	923
Avg (SD)				1122 (199)
5	300	2.68E-05	2.40E-08	1120
6	300	2.26E-05	2.00E-08	1131
7	300	2.71E-05	2.72E-08	998
Avg (SD)				1083 (67)
		Group 2 Total avg (SD)	1102 (136)	
Group 3				
2	400	4.46E-05	4.30E-08	1038
3	400	3.86E-05	5.23E-08	739
4	400	4.16E-05	5.97E-08	697
Avg (SD)		4.16E-05	5.14E-08	825 (186)
5	300	2.40E-05	3.30E-08	727
6	300	2.04E-05	2.47E-08	827
7	300	2.34E-05	2.54E-08	922
Avg (SD)				826 (98)
		Group 3 Total avg (SD)	825 (133)	
Bovine patellar cartilage by MSEN[1]		1030 (1090)		
Canine patellar cartilage by MSEN[2]		1070 (870)		

[1]Adams *et al*. [15].
[2]Chin-Purcell and Lewis [3].

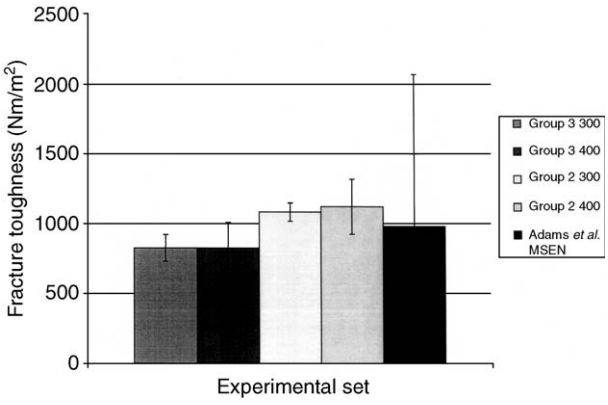

Figure 10 Fracture toughness predicted from power, power rate and Equation 3 for Groups 2 and 3 by micropenetration, and as measured by Adams *et al*. (1999) using an MSEN test. There is no statistically significant difference between any of the categories.

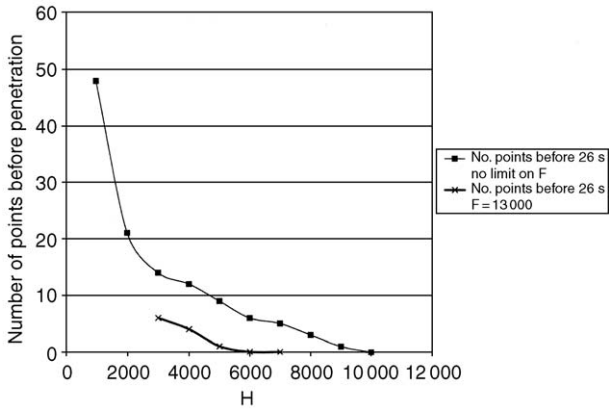

Figure 11 Effect of the value of H on the number of points classed as penetration before 26 s, the actual penetration point, with and without a limit on F. For $H > 5000\,mN\,nm/s^2$, one or less points for $t < 26$ s are classed as penetration if $F = 13\,000\,mN\,nm/s$. With no limit on F, many more points are classed as penetration, and consequently predicted penetration depth is greater. Limits on both power rate and power are necessary.

for both variation due to penetration and to noise. It is shown in the following that the predicted penetration depth is relatively insensitive to these limits.

The criterion for penetration depends on the factors H and F. The value of H was chosen based on examining the plots of power rate, to eliminate the inclusion of displacement points to penetration depth in the region where the power indicated there was no penetration, and to reduce the effects of noise. For example, for a 400 mN indent (Test 002), power vs. time indicated penetration occurred at about 26 s. Setting $H < 5000\,mN\,nm/s^2$ resulted in penetration predicted at multiple time points prior to 26 s, due to signal noise occasionally producing spikes in power rate. Setting H at $5000\,mN\,nm/s^2$ eliminated all but one point in the time range from 0 to 26 s. The number of penetration time points predicted prior to 26 s approached zero at $H = 5000$ (Fig. 11). The chosen H value satisfies the criterion that no displacement is included in penetration prior to the penetration point indicated by power vs. time. For $H = 5000$, variation in F showed that total predicted depth did not change for $F > 13\,000$ (Fig. 12). It must be appreciated, however, that this method for choosing H and F may be dependent on the specific noise levels of these tests and shapes of the power–time curves. Further work is needed to give greater confidence in use of these particular values of H and F and the fitting function.

Surface defect size provides an estimate of the volume of material evaluated by the test. The actual defect size for the 400 mN indents is approximately 200 μm deep × 230 μm at the surface, resulting in a crack area

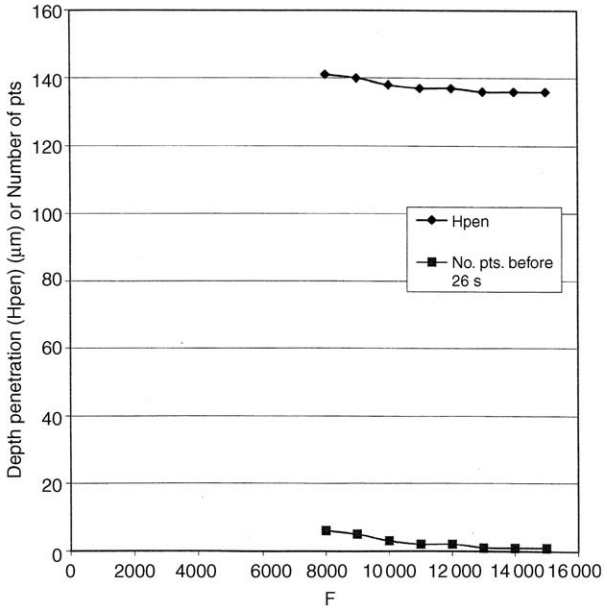

Figure 12 Effect of F on predicted penetration depth for $H = 5000$. There is no change in predicted penetration depth or number of points classed as penetration for $F > 13\,000$ mN nm/s, and relatively insensitive to F for $8000 < F$.

of approximately 460 μm^2. This is much smaller than specimen sizes used in conventional material tests of cartilage, but considerably larger than cartilage cells and extracellular matrix components. This volume will, of course, vary depending on tip geometry and penetration depth.

In defining the fracture toughness by Equation 5, it is assumed that the defect is conical and the corresponding crack surface area is approximately triangular. If the formed crack was exactly the shape of the cone, this would be a good estimate of crack area. This is not necessarily the case, however, as can be seen from the India ink images of the defects. There appear to be multiple cracks emanating from a central point (Figs. 2 and 4), although this varies with penetration depth. From viewing many penetration defects, it is evident that there is a wide variety of geometries of the surface defect caused by the indent. Some look like the highly oriented cracks seen when forming ''split lines'' by penetrating with a needle. Others are much less oriented, forming a nearly axisymmetric pattern. The shallower penetrations (300 mN) appear to be less oriented that the deeper penetrations (400 mN), perhaps reflecting the effect of the deeper tissue in forming the split lines. Dividing fracture work by one-half the cone penetrated area can also be thought of as a normalization procedure, similar to hardness, where the maximum load is divided by the projected defect area. In this case, the actual defect area is not directly important.

One question with the method is the effect of the tip geometry. In pilot work with a sharper 60° tip, the rapid change in power was much less evident. The blunt tip may be necessary to get the apparent instability and abrupt changes in power. Fibrillated cartilage also may not show the instability and rapid change in power as readily. Further study is needed to resolve this issue.

With only six indents in each of two specimens presented here, more testing is obviously needed. Work is in progress to increase these numbers and to assess the effect of alterations in material properties on the predicted fracture toughness. Efforts are also underway to quantify the effect of assumptions used in the methods and their limitations by performing model-based simulations of the penetration process. Also, the tests presented are for normal bovine cartilage. Tests must be performed on degenerating tissue to determine if softer tissue or tissue with disrupted surface can be tested with similar precision. Whether the methods in this paper can be applied to other viscoelastic materials with low stiffness must be determined.

Conclusions

A method for predicting the depth of penetration and fracture toughness of articular cartilage by micropenetration is presented. The predicted depth of penetration agrees well with depth determined by histology, and the predicted fracture toughness agrees well with tests done by macroscopic methods. The proposed methods are promising as a new method for measuring the failure properties of cartilage and other soft tissues and may be particularly applicable for use on specimens from small animals.

Acknowledgments

This work was supported primarily by the MRSEC Program of the National Science Foundation under Award Number DMR-9809364, and partially by the Catharine Mills Davis Endowment to the Department of Orthopaedic Surgery and a grant from the NIH (AR-14099). We are grateful to Anne Undersander, who prepared the histology sections.

References

1. P. PURSLOW, *J. Mater. Sci.* **18** (1983a) 3591.
2. P. PURSLOW, *J. Biomech.* **16** (1983b) 947.
3. M. CHIN-PURCELL and J. LEWIS, *J. Biomech. Eng.* **118** (1996) 545.
4. G. KEMPSON, in ''Adult Articular Cartilage,'' 2nd edn, edited by M. Freeman (Kent, UK, Pitman Medical Publishers, 1979), p. 333.
5. S. ROBERTS, B. WEIGHTMAN, J. URBAN and D. CHAPPELL, *J. Bone Joint Surg.* **68B** (1986) 278.
6. M. SCHMIDT, V. MOW, L. CHUN and D. EYRE, *J. Ortho. Res.* 8 (1990) 353.
7. J. CLARK and P. SIMONIAN, *Microscopy Res Tech.* **37** (1997) 299.
8. J. LEWIS and S. JOHNSON, *J. Anat.* **199** (2001) 483.
9. W. OLIVER and G. PHARR, *J. Mater. Res.* **7** (1992) 1564.
10. M. DOERNER and W. NIX, *ibid.* **1** (1986) 601.
11. G. KEMPSON, H. MUIR, C. POLLARD and M. TUKE, *Biochim. Biophys. Acta* **428** (1973) 741.
12. R. HORI and L. MOCKROS, *J. Biomech.* **9** (1976) 259.
13. V. MOW, M. GIBBS, W. LAI, W. ZHU and K. ATHANASIOU, *ibid.* **22** (1989) 853.
14. A. ATKINS and Y. MAI, ''Elastic and Plastic Fracture: Metals, Polymers, Ceramics, Composites, Biological Materials'' (John Wiley and Sons, NY, 1985).
15. D. ADAMS, K. BROSCHE and J. LEWIS, *Trans. 45th Orthop. Res. Soc.* (1999) 653.

Received 21 October 2002
and accepted 9 July 2003